

# A Superfluorinated Molecular Probe for Highly Sensitive *in Vivo* $^{19}\text{F}$ -MRI

Ilaria Tirotta,<sup>†,‡,¶</sup> Alfonso Mastropietro,<sup>§,¶</sup> Chiara Cordiglieri,<sup>∇,¶</sup> Lara Gazzera,<sup>†</sup> Fulvio Baggi,<sup>∇</sup> Giuseppe Baselli,<sup>||</sup> Maria Grazia Bruzzone,<sup>◆</sup> Ileana Zucca,<sup>§</sup> Gabriella Cavallo,<sup>†,‡</sup> Giancarlo Terraneo,<sup>†,‡</sup> Francesca Baldelli Bombelli,<sup>†,‡,⊥</sup> Pierangelo Metrangolo,<sup>\*,†,‡,♯</sup> and Giuseppe Resnati<sup>\*,†,‡</sup>

<sup>†</sup>Laboratory of Nanostructured Fluorinated Materials (NFMLab), Department of Chemistry, Materials, and Chemical Engineering “Giulio Natta”, <sup>‡</sup>Fondazione Centro Europeo Nanomedicina, and <sup>||</sup>Department of Electronics, Information, and Bioengineering, Politecnico di Milano, Milan, Italy

<sup>§</sup>Scientific Direction, <sup>∇</sup>Neurology IV Unit, and <sup>◆</sup>Neuroradiology Unit, Istituto Neurologico “CarloBesta”, Milan, Italy

<sup>⊥</sup>School of Pharmacy, University of East Anglia, Norwich, United Kingdom

<sup>♯</sup>VTT-Technical Research Centre of Finland, FI-02044 VTT, Espoo, Finland

**ABSTRACT:**  $^{19}\text{F}$ -MRI offers unique opportunities to image diseases and track cells and therapeutic agents *in vivo*. Herein we report a superfluorinated molecular probe, herein called PERFECTA, possessing excellent cellular compatibility, and whose spectral properties, relaxation times, and sensitivity are promising for *in vivo*  $^{19}\text{F}$ -MRI applications. The molecule, which bears 36 equivalent  $^{19}\text{F}$  atoms and shows a single intense resonance peak, is easily synthesized via a simple one-step reaction and is formulated in water with high stability using trivial reagents and methods.

In the ever more pressing quest for novel noninvasive tools for early disease diagnosis and treatment monitoring, magnetic resonance imaging (MRI) is one of the techniques that have gained more prominence in the last 20 years. In particular, outstanding results have been obtained in molecular imaging and cell tracking.<sup>1</sup> Due to its favorable magnetic properties and virtual absence in the human body,  $^{19}\text{F}$  nucleus has stood out as a valuable probe, which complements the wealth of information provided by  $^1\text{H}$  MRI, opening up a plethora of new possible applications.<sup>2</sup>

Several fluorinated contrast agents (CA) for *in vivo*  $^{19}\text{F}$ -MRI have been reported to date, most of which make use of liquid perfluorocarbons (PFC) or perfluoropolyethers (PFPE) generally administered as nanoemulsions of particle sizes around 100–200 nm.<sup>3</sup> However, the formulation of these perfluorinated CAs often requires the use of multiple surfactants and advanced dispersing devices.<sup>4</sup> Moreover, PFCs and PFPEs accumulate excessively in internal organs as there are no human enzymes and pathways known for their degradation *in vivo*.

The most used perfluorinated CAs in  $^{19}\text{F}$ -MRI are emulsions containing perfluorooctyl bromide (PFOB),<sup>5</sup> perfluoro[15]-crown-5ether (PF15C5E),<sup>6</sup> and a linear PFPE polymer mixture, commercialized as CellSense (CS; from Celsense, Inc.;<sup>7</sup> see Scheme S1). These three systems are the current standards used for preclinical and/or clinical studies, though

they are not optimal. For example, linear perfluorinated compounds giving more than one resonance frequency may induce chemical shift artifacts. On the other hand, the symmetrical PF15C5E is difficult to modify and, if covalently modified, would generate multiple  $^{19}\text{F}$  signals because its cyclic symmetry would then be broken. Importantly, both PF15C5E and CS require 3 h incubation to gain MRI-detectable cellular uptakes, with relevant repercussions on cell viability (PF15C5E: >80%; CS: ~80%).<sup>6,8</sup>

In order to overcome the existing gaps, we developed a superfluorinated molecular probe, herein called PERFECTA (from suPERfluorinatEdContrasT Agent; **1**; Figure 1), suitable

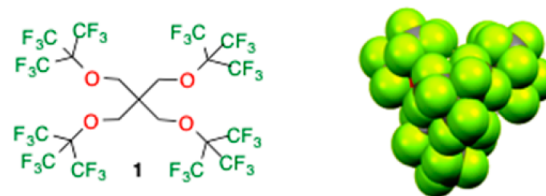


**Figure 1.** Chemical drawing (left) and single crystal X-ray structure of PERFECTA (**1**; right).

for *in vivo* cell tracking, characterized by a high detection sensitivity, a single and sharp resonance peak, good  $T_1$  and  $T_2$  values. Indeed, water formulation of PERFECTA showed excellent applicability for *in vivo*  $^{19}\text{F}$  MRI by imaging labeled dendritic cells (DCs), injected in naïve Lewis rats.

We designed PERFECTA with the objective of having as many equivalent  $^{19}\text{F}$  atoms as possible on a single and small molecular scaffold. As source of equivalent  $\text{CF}_3$  groups, perfluoro-*t*-butanol was used in analogy with Yu et al., who have synthesized various fluorocarbon dendrons containing up to 243 chemically identical F atoms.<sup>9</sup> In spite of this, no detailed report on the use in  $^{19}\text{F}$  MRI of the tetrasubstituted

**Received:** April 8, 2014

**Published:** June 2, 2014

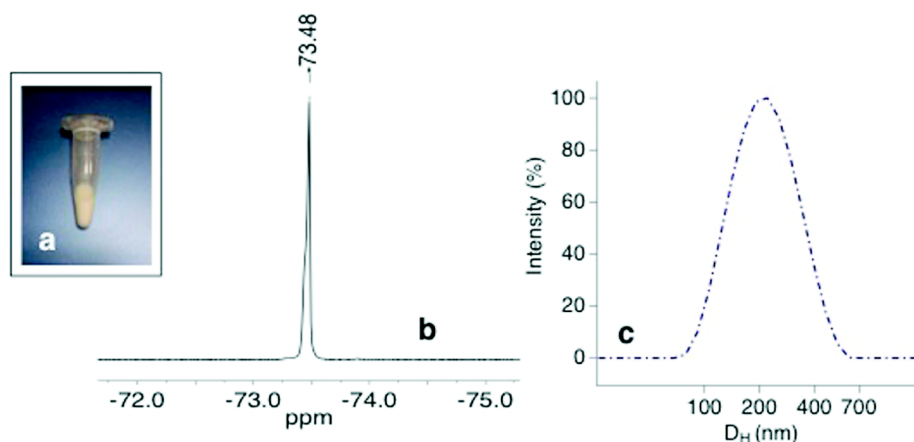


**Figure 2.** Characterization of a freshly prepared emulsion of PERFECTA: (a) Picture of an emulsion sample (74.40 mM in Milli-Q water); (b)  $^{19}\text{F}$ -NMR of a diluted sample in  $\text{D}_2\text{O}$  (12.40 mM); (c) intensity-weighted size distribution obtained from a DLS measurement using CONTIN analysis on a diluted sample (0.74 mM in Milli-Q water).

pentaerythritol derivative **1** has ever been reported in the scientific literature.<sup>10</sup>

PERFECTA was obtained in one step via a Mitsunobu reaction between pentaerythritol and perfluoro-*t*-butanol, which provided the desired product in good yield as a crystalline white powder insoluble in water and most common organic solvents (e.g., acetone, chloroform, methanol). Differently from PFOB, PF15C5E, and CS, PERFECTA is not perfluorinated but possesses a hydrocarbon polar core and four ether bonds, which might be subject of enzymatic degradation *in vivo*. However, X-ray diffraction analysis of single crystals of PERFECTA, obtained from 1,1,1,3,3,3-hexafluoroisopropanol, demonstrated that the polar core of the molecule is completely hindered by a fluorinated outer shell (Figure 1, right), thus making it a fluorous<sup>11</sup> nanodroplet.

A homogeneous, cloudy, off-yellow emulsion of PERFECTA, stable for weeks at room temperature, was easily obtained dispersing 75 mg in 1 mL of an aqueous solution containing 4% lecithin and 4% safflower oil (Figure 2a). This emulsion was characterized by  $^{19}\text{F}$ -NMR and dynamic light scattering (DLS) measurements (see SI). The  $^{19}\text{F}$ -NMR spectrum of the novel  $^{19}\text{F}$ -CA showed a sharp, very intense single peak at  $-73.48$  ppm (282.573 MHz at 7T, Figure 2b).  $^{19}\text{F}$ -NMR and  $^{19}\text{F}$ -MRI experiments, with both external and internal standards (see SI), led to estimate an average concentration of PERFECTA of  $74.40 \pm 1.98$  mM, corresponding to  $1.61 \pm 0.04 \times 10^{21}$   $^{19}\text{F}$  atoms per mL of emulsion.

DLS experiments showed monodisperse samples, for which a representative intensity-weighted size distribution is reported in Figure 3c. Nanoemulsion behavior in several fluids (water, PBS, cell culture media with or without fetal bovine serum and human plasma) was also evaluated, revealing high stability in all tested solutions with an averaged droplet size ranged between 140 and 220 nm (see Table SI2), and a polydispersity index (PDI)  $< 0.2$  (Table SI2). Emulsions showed a shelf life of about 6 weeks when kept at room temperature and 7 weeks at 4 °C (DLS analysis, Figures S5–S6).

After full physicochemical characterization, a series of experiments on phantoms were performed by using a 7T preclinical MRI system. A good signal to noise ratio (SNR) linearity ( $r^2 = 0.99$ ) was achieved by means of  $^{19}\text{F}$ -MRI at different concentrations in water (Figures 3a,b) and confirmed by quantitative  $^{19}\text{F}$ -NMR (Figure S7). Considering an

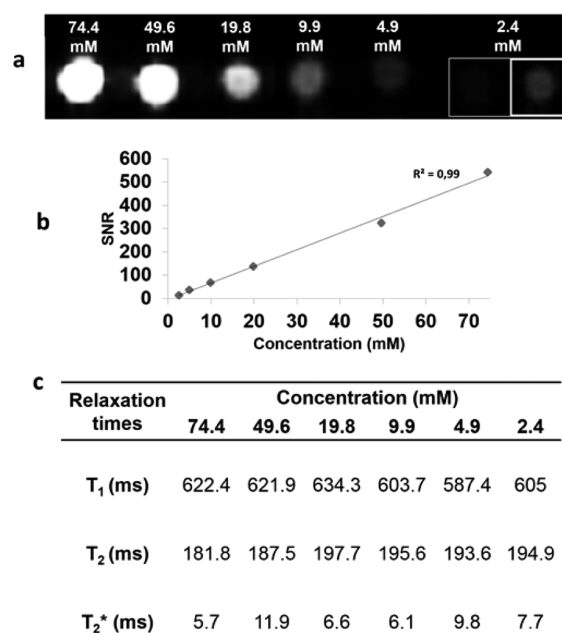


**Figure 3.** (a)  $^{19}\text{F}$ -MRI performed on phantoms containing nano-emulsion of PERFECTA diluted in water at different concentrations. In the box on the right the sample at the lowest concentration is shown after enhanced contrast for a better visualization. (b) SNR linearity and (c)  $T_1$ ,  $T_2$ , and  $T_2^*$  relaxation times estimated by  $^{19}\text{F}$ -MRI. For details on sequence parameters, please see SI.

acquisition time of about 1 h and a SNR of 3.5, we could estimate a detection threshold of about  $8.75 \times 10^{16}$   $^{19}\text{F}$  atoms per voxel. Analysis of  $T_1$  and  $T_2$  relaxation times on pure and diluted samples suggested the possibility of obtaining images with high SNR using fast sequences (high  $T_2$  values, Figure 3c).<sup>12</sup>

Cellular compatibility of the new  $^{19}\text{F}$ -CA was assessed on transformed hamster fibroblasts (BHK-21, Figure S9) and bone-marrow derived DCs from Lewis rat (Figure 4).<sup>13</sup> Nanoemulsion toxicity was evaluated with trypan blue staining to assess cell viability and with TUNEL fluorimetric reaction to analyze apoptosis induction (Figures 4a and S9). DCs viability (Figure 4b, top) and phenotype (Figure 4b, bottom) were also assessed by cytofluorimetry.<sup>14</sup> The nanoemulsions were perfectly compatible with cellular viability even at high

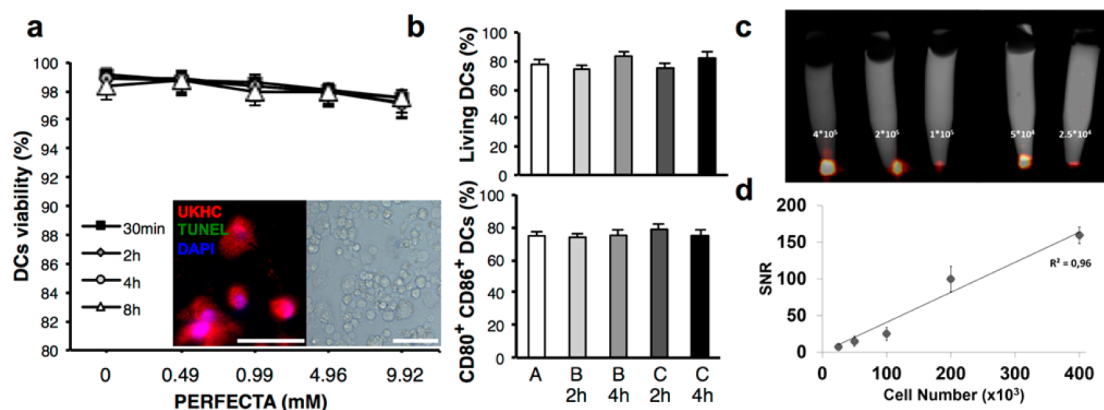


**Figure 4.** Analysis of nanoemulsion effect on viability and phenotype of bone-marrow derived DCs incubated with **PERFECTA** at increasing concentrations and at different incubation times. (a) Cell viability vs concentration of **PERFECTA** evaluated via fluorescence-apoptotic assay (TUNEL; left inserted image) and trypan blue exclusion (right inserted image), acquired via confocal and optical microscopy (magnification bars: 50  $\mu\text{m}$ ; UKHC: ubiquitous cytoskeletal kinesin; DAPI: nuclear marker). (b) Cytofluorimetric assays for living DCs (top graph) and CD80 and CD86 surface expression (bottom graph, CD80<sup>+</sup> CD86<sup>+</sup> percentage) on DCs incubated with control (A), nanoemulsions containing 2.48 (B) or 4.96 mM (C) of **PERFECTA**, for 2 and 4 h. Mean  $\pm$  SEM of duplicate samples from three independent experiments are shown. No statistically significant differences were found among samples (ANOVA). (c and d): *In vitro* <sup>19</sup>F-MRI on different amounts of <sup>19</sup>F-CA labeled DCs and SNR linearity assessment. Images in (c) are shown using different colorimetric scales to allow visualization.

concentration of **PERFECTA** (9.92 mM) and for long incubation periods (up to 8 h, Figure 4a). Moreover, the survival rate of DCs at 24 or 48 h following nanoemulsion exposure was evaluated via cytofluorimetry for living cells (Figure S11b, top) and for expression of surface DC markers (Figure S11b, bottom). No statistically significant difference among control (H<sub>2</sub>O, 4% lecithin, 4% safflower oil) and <sup>19</sup>F-CA labeled samples was observed. DCs exposed to the <sup>19</sup>F-CA did not change their phenotype nor alter immunomodulatory and activatory mRNAs expression, as evaluated by real time qPCR (Figure S11c).<sup>13</sup>

In order to evaluate the performance of the <sup>19</sup>F-CA *in vitro*, DCs labeled with the nanoemulsion were examined by <sup>19</sup>F-MRI.  $4 \times 10^5$  DCs were incubated for 2 and 4 h with different concentrations of **PERFECTA** (2.48 and 4.96 mM), and <sup>19</sup>F-MRI and <sup>19</sup>F-NMR were performed (Figure S10). Cells incubated at the higher concentration showed a more intense <sup>19</sup>F-MR signal (+30%), while incubation time did not significantly influence the cellular uptake, as proven by quantitative <sup>19</sup>F-NMR (up to  $1.92 \times 10^{13}$  <sup>19</sup>F atoms per cell). To assess the *in vitro* <sup>19</sup>F-MRI sensitivity, serial dilutions of <sup>19</sup>F-labeled DCs were analyzed. A detection threshold of  $9\text{--}10 \times 10^3$  DCs per voxel (1 voxel = 8.6  $\mu\text{L}$ ; concentration of  $\approx 10^6$  cells/mL) was estimated with an acquisition time of about 1 h (Figure 4c,d). Not only was the signal highly detectable but also persistent. Indeed <sup>19</sup>F-CA-labeled cells, cultured for further 5 days in fresh medium not containing <sup>19</sup>F-CA, were still detectable with a 40% of signal decrease (Figures S11d and S19). BHK cells behaved similarly to DCs (see SI).

Finally, to preliminarily assess feasibility of *in vivo* <sup>19</sup>F-MRI, we injected <sup>19</sup>F-CA-labeled DCs in naïve Lewis rats. Two different amounts of <sup>19</sup>F-DCs ( $5 \times 10^6$  and  $2 \times 10^6$ ) were injected in the subcutaneous popliteal area (right leg) and in the muscle (left leg; Figure 5a). 48 h after injection, the inoculated sites were evident in <sup>19</sup>F-MR images acquired with an acquisition time of 10 min and superimposed to anatomical <sup>1</sup>H-MR images (Figure 5b,c).

In conclusion, herein we report a new superfluorinated molecular probe for <sup>19</sup>F-MRI applications, **PERFECTA**, which bears 36 equivalent <sup>19</sup>F atoms and can be easily synthesized in

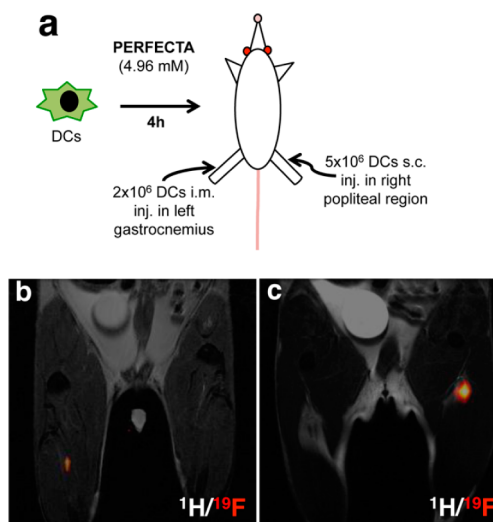


**Figure 5.** *In vivo* <sup>19</sup>F-MRI of <sup>19</sup>F-labeled DCs (4.96 mM of **PERFECTA**): (a)  $5 \times 10^6$  DCs injected subcutaneously (s.c.) in the right popliteal area and  $2 \times 10^6$  DCs injected intramuscularly (i.m.) in the left gastrocnemius; (b and c) *in vivo* <sup>1</sup>H/<sup>19</sup>F-MR images 48 h post injection.

good yield and large quantities through a simple one-step reaction starting from low-cost, commercially available reagents. Water-based nanoemulsions of the new probe (average droplet size ranged between 140 and 220 nm) can be easily obtained with trivial formulation methods and show excellent stabilities (over a month at both 4 °C and at room temperature).

With its very high fluorine concentration (2.68 M), the new <sup>19</sup>F-MRI CA shows a single intense resonance peak at both <sup>19</sup>F-NMR and MRI techniques, avoiding any possible artifact and misidentification. Its MRI performances, in terms of spectral properties, relaxation times, and SNRs, strongly indicate that the new <sup>19</sup>F-MRI CA is suitable for *in vivo* applications.

In fact, preliminary *in vivo* <sup>19</sup>F-MRI experiments demonstrated that labeled cells could be well detected in an acquisition time compatible with the safe permanence of the anesthetized animal inside the scanner (10 min). Furthermore,

PERFECTA shows high cellular compatibility (<5% cell death after 8 h incubation), as assessed on two different mammalian cell types. A short incubation time (2 h) is sufficient to guarantee cellular uptake of up to  $1.92 \times 10^{13}$   $^{19}\text{F}$  atoms per cell, which allows a detection threshold of  $<10^4$  DCs per voxel (1 voxel = 8.6  $\mu\text{L}$ ; concentration of  $\approx 10^6$  cells/mL) *in vitro*. Thus, we have demonstrated feasibility of *in vivo* use of a new superfluorinated CA, which we believe could easily be translated to preclinical applications.

## ■ ASSOCIATED CONTENT

### ● Supporting Information

Experimental procedures, further characterization, and images of spectra. This material is available free of charge via the Internet at <http://pubs.acs.org>.

## ■ AUTHOR INFORMATION

### Corresponding Authors

pierangelo.metrangolo@polimi.it

giuseppe.resnati@polimi.it

### Author Contributions

<sup>¶</sup>These authors contributed equally.

### Notes

The authors declare no competing financial interest.

## ■ ACKNOWLEDGMENTS

This work was funded by MIUR, FIRB project “FLUORIMAGING” no. RBAP1183B5. I.T., F.B.B., P.M., and G.R. are also thankful to Regione Lombardia (Fondo per lo Sviluppo e la Coesione - FAS 2007-2013) for additional financial support.

## ■ REFERENCES

- (1) (a) Hoehn, M.; Wiedermann, D.; Justicia, C.; Ramos-Cabrer, P.; Kruttwig, K.; Farr, T.; Himmelreich, U. *J. Physiol.* **2007**, *584*, 25. (b) L Villaraza, A. J.; Bumb, A.; Brechbiel, M. W. *Chem. Rev.* **2010**, *110*, 2921.
- (2) (a) Srinivas, M.; Boehm-Sturm, P.; Figdor, C. G.; de Vries, I. J.; Hoehn, M. *Biomaterials* **2012**, *33*, 8830. (b) Ruiz-Cabello, J.; Barnett, B. P.; Bottomley, P. A.; Bulte, J. W. M. *NMR Biomed.* **2010**, *24*, 114.
- (3) (a) Mulder, W. J. M.; McMahon, M. T.; Nicolay, K.; Ahrens, E. T.; Zhong, J. *NMR Biomed.* **2013**, *26*, 860. (b) Riess, J. G.; Krafft, M.-P. Fluorocarbon Emulsions as *in vivo* Oxygen Delivery Systems: Background and Chemistry. In *Blood Substitutes*; Winslow, R. M., Ed.; Academic Press, Oxford, 2006; Chapter 24, pp 259–275.
- (4) (a) Ruiz-Cabello, J.; Walczak, P.; Kedziorek, D. A.; Chacko, V. P.; Schmieder, A. H.; Wickline, S. A.; Lanza, G. M.; Bulte, J. W. M. *Magn. Res. Med.* **2008**, *60*, 1506. (b) Kimura, A.; Narazaki, M.; Kanazawa, Y.; Fujiwara, H. *Magn. Reson. Imag.* **2004**, *22*, 855.
- (5) Lanza, G. M.; Yu, X.; Winter, P. M.; Abendschein, D. R.; Karukstis, K. K.; Scott, M. J.; Chinen, L. K.; Fuhrhop, R. W.; Scherrer, D. E.; Wickline, S. A. *Circulation* **2002**, *106*, 2842.
- (6) Ahrens, E. T.; Flores, R.; Xu, H.; Morel, P. A. *Nat. Biotechnol.* **2005**, *23*, 983.
- (7) (a) Celsense, Inc. Home Page <http://www.celsense.com/> (accessed on March 21, 2014). (b) Janjic, J. M.; Srinivas, M.; Kadayakkara, D. K. K.; Ahrens, E. T. *J. Am. Chem. Soc.* **2008**, *130*, 2832.
- (8) Bonetto, F.; Srinivas, M.; Heerschap, A.; Mailliard, R.; Ahrens, E. T.; Figdor, C. G.; de Vries, I. J. M. *Int. J. Canc.* **2010**, *129*, 365.
- (9) (a) Jiang, Z.-X.; Liu, X.; Jeong, E.-K.; Yu, Y. B. *Angew. Chem., Int. Ed.* **2009**, *48*, 4755. (b) Yue, X.; Taraban, M. B.; Hyland, L. L.; Yu, Y. B. *J. Org. Chem.* **2012**, *77*, 8879.
- (10) Yu, Y.; Jiang, Z.-X. Highly Fluorinated Surfactants and Methods of Making and Using Same. U.S. Patent 8,252,778B2, August 28, 2012.
- (11) (a) Studer, A.; Hadida, S.; Ferritto, R.; Kim, S.-Y.; Jeger, P.; Wipf, P.; Curran, D. P. *Science* **1997**, *275*, 823. (b) Barthel-Rosa, L. P.; Gladysz, J. A. *Coord. Chem. Rev.* **1998**, *190*, 587. (c) Cametti, M.; Crousse, B.; Metrangolo, P.; Milani, R.; Resnati, G. *Chem. Soc. Rev.* **2011**, *41*, 31.
- (12) Mastropietro, A.; De Bernardi, E.; Breschi, G. L.; Zucca, I.; Cametti, M.; Soffientini, C. D.; de Curtis, M.; Terraneo, G.; Metrangolo, P.; Spreafico, R.; Resnati, G.; Baselli, G. *J. Magn. Reson. Imaging.* **2013**, DOI: 10.1002/jmri.24347.
- (13) Marolda, R.; Ruocco, C.; Cordiglieri, C.; Toscani, C.; Antozzi, C.; Mantegazza, R.; Baggi, F. *J. Neuroimmunol.* **2013**, *258*, 41.
- (14) Cordiglieri, C.; Marolda, R.; Franzi, S.; Cappelletti, C.; Giardina, C.; Motta, T.; Baggi, F.; Bernasconi, P.; Mantegazza, R.; Cavalcante, P. *J. Autoimmunity.* **2014**, DOI: 10.1016/j.jaut.2013.12.013.